A010

Solving the 3D Acoustic Wave Equation with Higher-order Mass-lumped Tetrahedral Finite Elements

E. Zhebel* (Shell Global Solutions International BV), S. Minisini (Shell Global Solutions International BV), A. Kononov (Source Contracting) & W. A. Mulder (Shell GSI BV / Delft University of Technology)

SUMMARY

Present-day computers allow for realistic 3D simulations of seismic wave propagation, as well as migration and inversion of seismic data with numerical solutions of the full wave equation. The finite-difference method is popular because of its simplicity but suffers from accuracy degradation for complex models with sharp interfaces between large impedance contrasts and for models with rough topography. A tetrahedral mesh offers more flexibility and maintains its accuracy if element boundaries are aligned with sharp interfaces. Higher-order finite elements with mass lumping provide a fully explicit time-stepping scheme. We have implemented elements of degree one, two, and three for the 3D acoustic wave equation. Numerical tests confirm the accuracy of the mass-lumped elements. There are two different third-degree elements that have almost the same accuracy, but one has a more favourable stability limit than the other. Convergence analysis shows that the higher the order of the element, the better the computational performance is. A low-storage implementation with OpenMP shows good scaling on 4-and 8-node platforms.

Introduction

The wave equation in the time domain is traditionally solved by the finite-difference method, which is relatively easy to implement and parallelize. For problems with complex geometries and strong heterogeneities, the finite-element method is better suited. In particular, tetrahedra offer the flexibility to fit element boundaries to the sharp interfaces between materials with different properties. Unfortunately, the standard finite-element method requires solution of the large sparse linear system of equation that represents the mass matrix. Tordjman (1995) (Cohen et al., 1995, 2001) proposed the use of mass lumping, replacing the mass matrix by a diagonal matrix. This results in a fully explicit time-stepping method. The mass-lumped finite elements should obey the following requirements: conformity, symmetric arrangement of nodes, positive integration weights, and the same order of accuracy as elements without mass lumping (Chin-Joe-Kong et al., 1999). For their construction, the standard finite element of a certain degree M is enriched with higher order polynomials that reduce to degree M on the edges. The extra degrees of freedom should enable the construction of sufficiently accurate integration rule that allows mass lumping without loss of accuracy. The standard second-order linear element ($M = 1$) fits these requirements in 2D and 3D. In 2D, the quadratic triangular element ($M = 2$) enriched by a cubic bubble function (Fried and Malkus, 1975) is the one with the smallest number of nodes. Tordjman (1995) found a cubic triangular element ($M = 3$). Higher order elements were found by Mulder (1996) ($M = 4$), Chin-Joe-Kong et al. (1999) ($M = 5$) and Giraldo and Taylor (2006) ($M = 6, 7$). Mulder (1996) made the extension of this idea to 3D for the quadratic tetrahedral element ($M = 2$) by adding polynomial bubble functions of degree 4 to the faces ($M_f = 4$) and the interior ($M_i = 4$), resulting in 23 points per element. Later on, Chin-Joe-Kong et al. (1999) considered cubic elements and found two different ones with the desired properties ($M = 3$, $M_f = 5$, $M_i = 6$; 50 points per element).

Here, we present an implementation of these 3D higher-order tetrahedral finite elements with mass lumping and investigate their accuracy and performance.

Implementation details

We want to solve the constant-density acoustic wave equation

$$\frac{1}{c^2(\mathbf{x})}\frac{\partial^2 p(t,\mathbf{x})}{\partial^2 t} - \Delta p(t,\mathbf{x}) = s(t,\mathbf{x}) \tag{1}$$

with pressure $p(t,\mathbf{x})$ depending on time t and position $\mathbf{x}$, sound speed $c(\mathbf{x})$ and source term $s(t,\mathbf{x})$, $\mathbf{x} \in \Omega \subset \mathbb{R}^3$. The natural (van Neumann) boundary conditions are considered. The weak formulation of this problem is

$$\int_\Omega \left[c^{-2}\frac{\partial^2 p}{\partial^2 t} v + \nabla_{\mathbf{x}} u \cdot \nabla_{\mathbf{x}} v - sv \right] d\mathbf{x} = 0, \tag{2}$$

for all test functions $v \in H_0^1(\Omega)$. The discretization of (2) with the finite-element method leads to

$$\mathbf{p}^{n+1} = 2\mathbf{p}^n - \mathbf{p}^{n-1} + \Delta t^2 \mathscr{L}\mathbf{p}^n, \quad \mathscr{L} = \mathscr{M}_h^{-1}\left(-\mathscr{K}_h\,\mathbf{p}^n + \mathbf{s}^n\right), \tag{3}$$

if standard second-order time stepping is chosen. Higher-order time stepping is straight-forward (Dablain, 1986; Shubin and Bell, 1987). $\mathscr{M}_h$ is the mass matrix, $\mathscr{K}_h$ the stiffness matrix and $\mathbf{s}$ is discrete source term. The superscript counts the time steps.
Let $\xi_i, i = 0,\ldots,3$, with $\xi_0 = 1 - \xi_1 - \xi_2 - \xi_3$ be the barycentric coordinates on each reference tetrahedron. Then the contribution of each element τ_m to the mass matrix $\mathscr{M}_h$ is $c_m^{-2}\,\det(J_m)A$, where J_m is Jacobian of the coordinate transformation and $A_{k,l} = \int_{\tilde{\tau}} \phi_k \phi_l d\xi_1 d\xi_2 d\xi_3$ is evaluated on the reference element $\tilde{\tau}$ with shape functions $\phi_k(\xi)$, $k = 1,\ldots,n$. On each element, shape functions are defined as Lagrangian polynomials that equal 1 on one of the nodes and 0 on the other nodes. The polynomials are chosen in such a way that mass lumping can be applied without loss of accuracy. That means that polynomials up to degree $q = M + \max(M, M_f, M_i) - 2$ should be integrated exactly by numerical quadrature,

M	type	CFL
1		1.18
2		0.090
3	1	0.059
3	2	0.105

Table 1 *Values of* CFL *based on the spectral radius for a single reference element, for various mass-lumped elements of degree M. These numbers represent estimates of the constant in the stability condition.*

for shape functions of a maximum degree M and additional degrees M_f and M_i. If mass lumping is used, the matrix A is replaced by a diagonal matrix obtained from row sums $\bar{A}_{k,k} = \sum_{l=1}^{n} A_{k,l}$. Before starting the time steps, the inverse mass matrix is computed. To save storage, the stiffness matrices are recomputed in each time step. The contribution to the stiffness matrix for each tetrahedron τ_m is $\sum_{k,l} C^m_{k,l} B^{k,l}$, where $B^{k,l}_{i,j} = \int_{\tilde{\tau}} \frac{\partial \phi_i}{\partial \xi_k} \cdot \frac{\partial \phi_j}{\partial \xi_l} d\xi_1 d\xi_2 d\xi_3$ and $C^m_{k,l}$ are the entries of $C^m = \det(J_m)^{-1} J_m^{-1} J_m^{-\mathsf{T}}$. The matrices $B^{k,l}$ on the reference tetrahedron remain fixed and are hardcoded in the programme. Note that $B^{k,l}_{i,j} = B^{l,k}_{j,i}$, which together with the symmetry of C^m is used to reduce the number of operations. The contribution to the time step becomes

$$a_i \sum_{k=1}^{3} \left[C^m_{k,k} \sum_j B^{k,k}_{i,j} p^n_j + \sum_{l=k+1}^{3} C^m_{k,l} \sum_j \left(B^{k,l}_{i,j} + B^{l,k}_{i,j} \right) p^n_j \right], \tag{4}$$

where a_i contains the inverse of the diagonal mass matrix and other factors. In our implementation, the global stiffness matrix is never formed. We only store the wavefield at two time levels, reusing the storage of $\mathbf{p}^{n-1}$ for $\mathbf{p}^{n+1}$, the diagonal inverted mass matrix of the same size, and a single pointer table for the local to global map.

For the simplest element, $M = 1$, it is more efficient to directly evaluate the contribution of the stiffness matrix for each element rather than using precomputed matrices $B^{k,l}$. In that case, we end up with a contribution of the form $(6 \det(J_m))^{-1} G_m G_m^{\mathsf{T}} \mathbf{p}^n$ per element τ_m, where $G_m^{\mathsf{T}} = \big((\mathbf{x}_3 - \mathbf{x}_1) \times (\mathbf{x}_2 - \mathbf{x}_1) \;\; (\mathbf{x}_2 - \mathbf{x}_0) \times (\mathbf{x}_3 - \mathbf{x}_0) \;\; (\mathbf{x}_3 - \mathbf{x}_0) \times (\mathbf{x}_1 - \mathbf{x}_0) \;\; (\mathbf{x}_1 - \mathbf{x}_0) \times (\mathbf{x}_2 - \mathbf{x}_0) \big)$.

The second-order time-stepping scheme is stable if $(\Delta t)^2 \leq 4/\lambda_{\max}(\mathscr{L})$, with $\lambda_{\max}(\mathscr{L})$ the spectral radius of $\mathscr{L}$ from (3). A crude estimate is $\Delta t \leq (d/c)_{\min}$ CFL with $\mathtt{CFL} = 2/\left(d^{(0)} \lambda^{(0)}_{\max} \right)^{1/2}$ where $(d/c)_{\min}$ is the minimum ratio over all elements of the radius d of the inscribed sphere and the velocity. Here $\lambda^{(0)}_{\max} = \lambda_{\max}\left(A^{-1} \sum_{k=1}^{3} B^{k,k} \right)$ is computed on a single reference tetrahedron with natural boundary conditions, having $d^{(0)} = 1 - 1/\sqrt{3}$. Table 1 provides these constants for a number of different types of elements. The second cubic element – $M = 3$, type 2, see Table 24 of Chin-Joe-Kong et al. (1999) – has a more favourable stability limit than the first.

For higher-order elements, an OpenMP parallelization of the last expression yielded good speed-ups on 4- and 8-core platforms, see Table 2.

cores	efficiency	
	$M = 2$	$M = 3 (2)$
4	0.87	0.92
8	0.61	0.85

Table 2 *OpenMP efficiency, the ratio of measured elapsed time on one core to number of cores multiplied by elapsed time on those cores, for elements of degree 2 and 3 (type 2).*

Results

We start with accuracy tests for a constant velocity model and an explosive source. To avoid problems with the source representation and absorbing boundary conditions, we consider the initial value problem with natural boundary condition. The domain is a cube with sides of 2 km, the velocity is 1 km/s. The wavelet is the second derivative of $[1 - (2t/T_w)^2]^8$ for $|t| \leq T_w/2$ and zero otherwise. The duration of the

wavelet T_w is 0.4s in this example. We start the computation at a time of 0.3s and stop it at 0.75s when the wave approaches the boundary. Figure 1 shows results for second- and fourth-order time stepping on increasingly finer grids. The errors at the end of the computation were computed by the maximum norm (dashed lines) over all element nodes and by the L_2-norm (drawn lines). The integral over the domain for L_2 norm was computed with the numerical integration weights obtained with the mass lumping. The errors were normalized by the maximum value of the exact solution. Both second- and fourth-order time schemes ran at 75% of the maximum time step, which for the fourth-order scheme is larger than the second-order scheme by a factor $\sqrt{3}$. With fourth-order time stepping, the errors show the expected accuracy behaviour as h^{M+1}, with h a length scale proportional to $N^{-1/3}$ and N the number of degrees of freedom or solution values at one time step. For the $M = 3$ elements the second-order time-stepping error starts to show lower-order behaviour on finer grids (larger N). The pictures on the right show that higher-degree elements are more efficient than those of lower degree in spite of the additional cost per element, except perhaps if one is willing to accept a fairly large error. This is similar to the 2D case (Mulder, 1996).

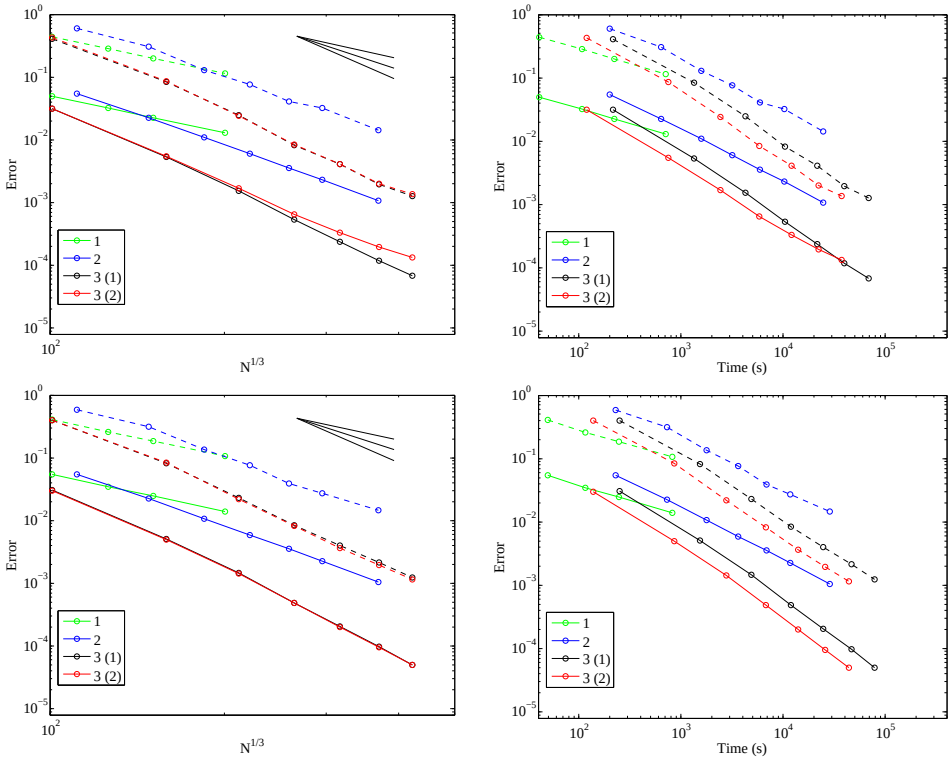

Figure 1 *Error as a function of the degrees of freedom N to the power $1/3$ (left) and computer time used (right) for degrees $M = 1$, 2, and 3, respectively. For the last, the two different elements produce nearly the same errors. The two lines for each degree mark the maximum error (dashed) and its 2-norm (drawn), the last being always smaller. The three black lines next to the legend in the picture on the left-hand side have slopes of $-(M+1)$, equal to the power of the expected spatial discretization error. The top row shows results for second-order and the bottom row for fourth-order time stepping with a time step based on 75% of the maximum CFL number.*

The Interior-Penalty Discontinuous Galerkin (IP-DG) method (De Basabe et al., 2008) has $(M+1)(M+2)(M+3)/6$ nodes per element, less than the mass lumped elements, but nodes are not shared among neighbours. For $M = 2$, IP-DG has 10 nodes per element, whereas the mass-lumped element with 23 nodes per element effectively has around 8.5 nodes per element for a typical mesh. We therefore expect the mass-lumped elements to be more efficient. For $M = 3$, we have 20 nodes for IP-DG and around 25 for mass lumping. In that case, it needs to be seen which element is more efficient, because, although IP-DG requires less nodes, it involves additional flux computations. Note that IP-DG has the advantage of going to arbitrary high order and offers more gridding flexibility.

Figure 2 shows a cut through the mesh and a vertical cross section of the wavefield for a simple example with an ellipsoidal high-velocity region. Ideally, the diameters of the tetrahedra scale with the local velocity. In that way, the number of points per wavelength as well as the stability requirements are the more or less the same in each element.

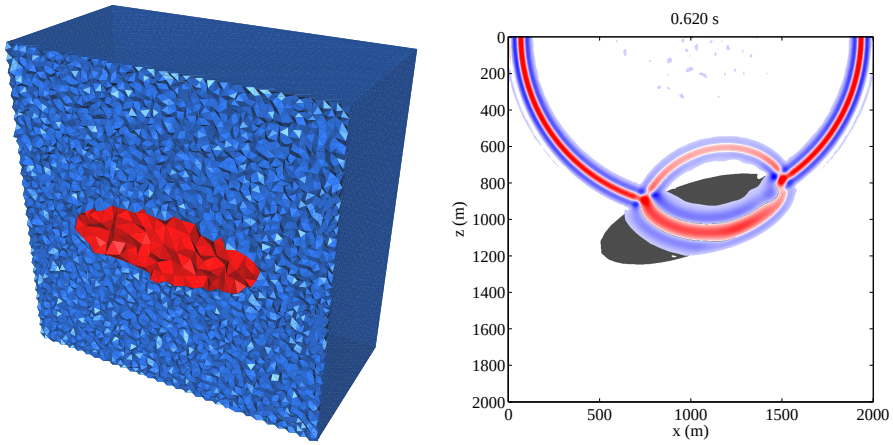

Figure 2 *Example of a tetrahedral mesh (left) and a vertical cross section of the wavefield (right) generated by an explosive source just below the free surface in a constant velocity model with an ellipsoidal high-velocity volume.*

Conclusions

Higher-order mass-lumped tetrahedral elements allow for flexible and accurate modelling of complex subsurface models and topography. They resemble explicit finite-difference methods both in terms of time stepping and in ease of parallelization, but are more accurate in their representation of sharp interfaces between materials of different impedance if the element boundaries follow the interfaces. Accuracy tests confirm the expected scaling of the numerical errors with element diameter. Quadratic continuous elements should be more efficient that their IP-DG counterpart. For cubic elements, we expect them to be competitive. For higher degrees, continuous elements have not yet been determined.

References

Chin-Joe-Kong, M.J.S., Mulder, W.A. and van Veldhuizen, M. [1999] Higher-order triangular and tetrahedral finite elements with mass lumping for solving the wave equation. *Journal of Engineering Mathematics*, **35**, 405–426, doi:10.1023/A:1004420829610.

Cohen, G., Joly, P., Roberts, J.E. and Tordjman, N. [2001] Higher order triangular finite elements with mass lumping for the wave equation. *SIAM Journal on Numerical Analysis*, **38**(6), 2047–2078, doi: 10.1137/S0036142997329554.

Cohen, G., Joly, P. and Tordjman, N. [1995] Higher order triangular finite elements with mass lumping for the wave equation. *Proceedings of the Third International Conference on Mathematical and Numerical Aspects of Wave Propagation*, SIAM, Philadelphia, 270–279.

Dablain, M.A. [1986] The application of high-order differencing to the scalar wave equation. *Geophysics*, **51**(1), 54–66, doi:10.1190/1.1442040.

De Basabe, J.D., Sen, M.K. and Wheeler, M.F. [2008] The interior penalty discontinuous Galerkin method for elastic wave propagation: grid dispersion. *Geophysical Journal International*, **175**(1), 83–93, doi:10.1111/j.1365-246X.2008.03915.x.

Fried, I. and Malkus, D.S. [1975] Finite element mass matrix lumping by numerical integration with no convergence rate loss. *Int. J. Solids Structures*, **11**, 461–466.

Giraldo, F.X. and Taylor, M.A. [2006] A diagonal-mass-matrix triangular-spectral-element method based on cubature points. *Journal of Engineering Mathematics*, **56**(3), 307–322, doi:10.1007/s10665-006-9085-7.

Mulder, W.A. [1996] A comparison between higher-order finite elements and finite differences for solving the wave equation. *Proceedings of the Second ECCOMAS Conference on Numerical Methods in Engineering*, John Wiley & Sons, Chichester, 344–350.

Shubin, G.R. and Bell, J.B. [1987] A modified equation approach to constructing fourth order methods for acoustic wave propagation. *SIAM Journal on Scientific and Statistical Computing*, **8**(2), 135–151, doi:10.1137/0908026.

Tordjman, N. [1995] *Élements finis d'order élevé avec condensation de masse pour l'equation des ondes*. Ph.D. thesis, L'Université Paris IX Dauphine.